ANALYSIS OF INTERNAL SUBLOOPS DUE TO INCOMPLETE PHASE TRANSFORMATIONS IN SHAPE MEMORY ALLOYS

Marcelo Amorim Savi
Alberto Paiva
Universidade Federal do Rio de Janeiro
COPPE – Departamento de Engenharia Mecânica
Centro de Tecnologia – Sala G-204, Caixa Postal 68.503
21.945.970 – Rio de Janeiro – R.J. – Brasil
savi@ufrj.br paiva@lavi.coppe.ufrj.br

Abstract. *The hysteretic response of shape memory alloys (SMAs) is one of their essential characteristics related to the martensitic phase transformation. Basically, the hysteresis loop may be observed in both stress-strain and strain-temperature curves. It is possible to define the major (or external) hysteresis loop as the envelope of all minor (or internal) hysteresis loops, usually denoted as subloops. The macroscopic description of the SMA hysteresis loops, together with their subloops due to incomplete phase transformations, is an important feature in the phenomenological analysis of the thermomechanical behavior of SMAs, arising great interest for technological applications. This contribution exploits these internal subloops employing a one-dimensional constitutive model with internal constraints. Comparisons between numerical and experimental results show that they are in close agreement. Moreover, numerical simulations are carried out elucidating different aspects related to this hysteretic behavior, showing the capability of the model to describe these inner subloops.*

Keywords*: Shape Memory Alloy, constitutive model, subloops, numerical simulation.*

1. Introduction

Shape Memory Alloys (SMAs) are metallic alloys able to recover their original shape (or to develop large reaction forces when they have their recovery restricted) through the imposition of a temperature and/or a stress field, due to phase transformations the material undergoes. Their remarkable properties are attracting much technological interest, motivating different applications in several fields of science and engineering.

SMAs present complex thermomechanical behaviors related to different physical processes, which turn their description extremely difficult. The main phenomena related to these alloys from macroscopic point of view are: pseudoelasticity, shape memory effect, which may be one-way (SME) or two-way (TWSME), and phase transformation due to temperature variation. All these behaviors present a hysteretic response associated to each phase transformation, which is mainly caused by frictional effects arisen from interfaces movement involving austenite and martensite (phase transformation) or twinned and detwinned martensite (reorientation process). This hysteretic feature may be either stress induced as seen in stress-strain diagrams or temperature induced as seen in strain-temperature diagrams. When complete phase transformation takes place, the (external) hysteresis loop formed can be defined as the envelope of all minor (internal) hysteresis loops, usually denoted as subloops (Bo & Lagoudas, 1999).

Literature reports many efforts related to the SMA hysteresis loops analysis, from either theoretical or experimental points of view. Muller & Xu (1991) present a study on the pseudoelastic behavior of SMAs, exploiting the description of inner subloops. The authors propose a constitutive model based on the polynomial Landau-Devonshire theory, which considers that states inside the hysteresis loop are metastable. Their work compares results obtained with the proposed model with those obtained by experimental tests and show good qualitative agreement. Ortin (1991) revisits the description of SMAs subloops considering the Preisach model. Again, the proposed model captures the general behavior of internal subloops related to pseudoelasticity. Tanaka *et al.* (1995) analyze subloops related to both stress-strain and strain-temperature curves. The proposed model is based on the model with assumed phase transformation kinetics previously presented in Tanaka & Nagaki (1982). After that, other models with assumed phase transformation kinetics were employed in order to describe the thermomechanical behavior of internal subloops. Brinson & Huang (1996) present some results that show the capability of these models to describe internal subloops.

Different features about subloops are also treated in Tanaka *et al.* (1996), where a discussion about plateaus on stress-strain hysteresis in SMAs is carried out. Bo & Lagoudas (1999) present a phenomenological model using information based on the Preisach model in order to correctly account minor hysteresis loops. Comparisons between the cited model predictions and the experimental results show that it can describe the minor loop hysteresis related to the strain-temperature response of SMAs.

This contribution exploits the description of the internal subloops due to incomplete phase transformation related to the thermomechanical response of SMAs employing a constitutive model previously proposed by Paiva *et al.* (2005). Comparisons between numerical and experimental results show that they are in close agreement, which reveal the model capability to describe pseudoelastic subloops. Moreover, numerical simulations are carried out, attesting that the model is able to capture thermal subloops besides stress-induced subloops.

2. Constitutive Model

There are different ways to describe the thermomechanical behavior of SMAs (Paiva & Savi, 2004). Here, a constitutive model that is built upon the Fremond's model (Fremond, 1987, 1996) and previously presented in different references (Savi *et al.*, 2002, Baêta-Neves *et al.*, 2004, Paiva *et al.*, 2005) is employed. This model considers different material properties and four macroscopic phases for the description of the SMA behavior. The model also considers plastic strains and plastic-phase transformation coupling, which turns possible the two-way shape memory effect description. Moreover, tensile-compressive asymmetry is taken into account.

The model formulation considers, besides elastic strain (ε_e) and temperature (T), four more state variables associated with the volumetric fraction of each macroscopic phase considered. β_1 is associated with tensile detwinned martensite, β_2 is related to compressive detwinned martensite, β_3 represents austenite and β_4 corresponds to twinned martensite. A free energy potential is proposed concerning each isolated phase. After this definition, a free energy of the mixture can be written weighting each energy function with its volumetric fraction. Since $\beta_1 + \beta_2 + \beta_3 + \beta_4 = 1$, it is possible to rewrite the free energy of the mixture as a function of three volumetric fractions: β_n (n = 1,2,3). After this, it is assumed an additive decomposition where the elastic strain may be written as: $\varepsilon_e = \varepsilon - \varepsilon_p - \alpha_h (\beta_1 - \beta_2)$. Parameter α_h is introduced in order to define the horizontal width of the stress-strain hysteresis loop, while α helps vertical hysteresis loop control on stress-strain diagrams. A pseudo-potential of dissipation is defined as a function of the state variables rates $\dot{\varepsilon}$, $\dot{T}$ and $\dot{\beta}_n$ (n = 1,2,3). By employing the standard generalized material approach (Lemaitre & Chaboche, 1990), it is possible to obtain a complete set of constitutive equations that describes the thermomechanical behavior of SMAs as presented bellow:

$$\sigma = E\left(\varepsilon - \varepsilon_p\right) + \left(\alpha^C + E\alpha_h^C\right)\beta_2 - \left(\alpha^T + E\alpha_h^T\right)\beta_1 - \Omega\left(T - T_0\right) \tag{1}$$

$$\dot{\beta}_1 = \frac{1}{\eta_1}\left\{ \alpha^T\left(\varepsilon - \varepsilon_p\right) + \Lambda_1 + \left(\alpha_h^C\alpha^T + \alpha_h^T\alpha^C + E\alpha_h^T\alpha_h^C\right)\beta_2 - \left(2\alpha_h^T\alpha^T + E\alpha_h^{T\,2}\right)\beta_1 + \right.$$
$$\left. + \alpha_h^T\left[E\left(\varepsilon - \varepsilon_p\right) - \Omega\left(T - T_0\right)\right] - \eta_{ci}K\gamma - \eta_{ck}\frac{\mu}{H} - \partial_1 J_\pi \right\} + \partial_1 J_\chi \tag{2}$$

$$\dot{\beta}_2 = \frac{1}{\eta_2}\left\{ -\alpha^C\left(\varepsilon - \varepsilon_p\right) + \Lambda_2 + \left(\alpha_h^T\alpha^C + \alpha_h^C\alpha^T + E\alpha_h^C\alpha_h^T\right)\beta_1 - \left(2\alpha_h^C\alpha^C + E\alpha_h^{C\,2}\right)\beta_2 \right.$$
$$\left. - \alpha_h^C\left[E\left(\varepsilon - \varepsilon_p\right) - \Omega\left(T - T_0\right)\right] - \eta_{ci}K\gamma - \eta_{ck}\frac{\mu}{H} - \partial_2 J_\pi \right\} + \partial_2 J_\chi \tag{3}$$

$$\dot{\beta}_3 = \frac{1}{\eta_3}\left\{ -\frac{1}{2}\left(E_A - E_M\right)\left(\varepsilon - \varepsilon_p + \alpha_h^C\beta_2 - \alpha_h^T\beta_1\right)^2 + \Lambda_3 + \left(\Omega_A - \Omega_M\right)\left(T - T_0\right)\left(\varepsilon - \varepsilon_p + \alpha_h^C\beta_2 - \alpha_h^T\beta_1\right) - \right.$$
$$\left. - \frac{1}{2}\left(K_A - K_M\right)\gamma^2 - \left(\frac{1}{2H_A} - \frac{1}{2H_M}\right)\mu^2 + \eta_{ci}K\gamma + \eta_{ck}\frac{\mu}{H} - \partial_3 J_\pi \right\} + \partial_3 J_\chi \tag{4}$$

$$\dot{\varepsilon}_p = \lambda\ \mathrm{sign}\left(\sigma - \mu\right) \tag{5}$$

$$\dot{\gamma} = \left|\dot{\varepsilon}_p\right| + \eta_{ci}\left(\dot{\beta}_1 + \dot{\beta}_2 - \dot{\beta}_3\right) \tag{6}$$

$$\dot{\mu} = H\dot{\varepsilon}_p + \eta_{ck}\left(\dot{\beta}_1 + \dot{\beta}_2 - \dot{\beta}_3\right) \tag{7}$$

where $E = E_M + \beta_3 (E_A - E_M)$ is the elastic modulus while $\Omega = \Omega_M + \beta_3 (\Omega_A - \Omega_M)$ is related to the thermal expansion coefficient. Moreover, $K = K_M + \beta_3 (K_A - K_M)$ is the plastic modulus and $\frac{1}{H} = \frac{1}{H_M} - \beta_3\left(\frac{1}{H_M} - \frac{1}{H_A}\right)$ is the kinematic hardening modulus. Notice that subscript "A" refers to austenitic phase, while "M" refers to martensite. Besides, different properties are assumed to consider tension-compression asymmetry, where the superscript "T" refers to tensile while "C" is related to compressive properties. Moreover, parameters Λ_1, Λ_2 and Λ_3 are associated with phase

transformations stress levels and are temperature dependent as follows: $\Lambda_1 = -L_0^T + \frac{L^T}{T_M}(T - T_M)$; $\Lambda_2 = -L_0^C + \frac{L^C}{T_M}(T - T_M)$ and $\Lambda_3 = -L_0^A + \frac{L^A}{T_M}(T - T_M)$, where T_M is the temperature below which the martensitic phase becomes stable, while L_0^T, L^T, L_0^C, L^C, L_0^A and L^A are parameters related to critical stress for the various phase transformations.

The terms $\partial_n J_\pi$ (n = 1,2,3) corresponds to the sub-differentials of the indicator function J_π with respect to β_n (Rockafellar, 1970). The indicator function $J_\pi(\beta_1, \beta_2, \beta_3)$ is related to the following convex set π, which provides the internal constraints related to the phases' coexistence.

$$\pi = \left\{ \beta_n \in \Re \,\middle|\, 0 \le \beta_n \le 1; \quad \beta_1 + \beta_2 + \beta_3 \le 1 \right\} \tag{8}$$

With respect to the evolution equations of volumetric fractions, η_1, η_2 and η_3 represent the internal dissipation related to phase transformations. Moreover $\partial_n J_\chi$ (n = 1,2,3) are the sub-differentials of the indicator function J_χ with respect to $\dot{\beta}_n$ (Rockafellar, 1970). This indicator function related to the convex set χ, establishes conditions for the correct description of internal sub-loops due to incomplete phase transformations and also avoids phase transformations of the type: $M+ \Rightarrow M$ or $M- \Rightarrow M$. Hence, the convex set χ may be written as follows for a mechanical loading history with $\dot{\sigma} \neq 0$:

$$\chi = \left\{ \dot{\beta}_n \in \Re \,\middle|\, \begin{array}{l} \dot{\varepsilon}\,\dot{\beta}_1 \ge 0; \quad \dot{\varepsilon}\,\dot{\beta}_3 \le 0 \quad \text{if} \quad \varepsilon_0 > 0 \\ \dot{\varepsilon}\,\dot{\beta}_2 \le 0; \quad \dot{\varepsilon}\,\dot{\beta}_3 \ge 0 \quad \text{if} \quad \varepsilon_0 < 0 \end{array} \right\} \tag{9}$$

On the other hand, when $\dot{\sigma} = 0$, the convex set χ is expressed by:

$$\chi = \left\{ \dot{\beta}_n \in \Re \,\middle|\, \begin{array}{l} \dot{T}\,\dot{\beta}_1 \begin{cases} < 0 \text{ if } \dot{T} > 0, \sigma < \sigma_{\mathrm{M}}^{\mathrm{crit}} \text{ and } \beta_1^s \neq 0 \\ = 0 \text{ otherwise} \end{cases}; \\ \dot{T}\,\dot{\beta}_2 \begin{cases} < 0 \text{ if } \dot{T} > 0, \sigma < \sigma_{\mathrm{M}}^{\mathrm{crit}} \text{ and } \beta_2^s \neq 0 \\ = 0 \text{ otherwise} \end{cases}; \\ \dot{T}\,\dot{\beta}_3 \ge 0 \\ -\dot{\beta}_1^2 - \dot{\beta}_1\dot{\beta}_3 = 0 \quad \text{or} \quad -\dot{\beta}_2^2 - \dot{\beta}_2\dot{\beta}_3 = 0 \end{array} \right\} \tag{10}$$

where $\varepsilon_0 = \varepsilon - \frac{\Omega}{E}(T - T_0)$ and β_1^s, β_2^s are the values of β_1 and β_2, respectively, when the phase transformation begins to take place. Moreover, σ_M^{crit}, which actually has different values for tensile and compressive behaviors, are the critical stress values for $M \Rightarrow M+$ and $M \Rightarrow M-$ phase transformations, respectively $\sigma_M^{T\,\mathrm{crit}}$ and $\sigma_M^{C\,\mathrm{crit}}$. For more detailed information about how to analytically obtain the parameters σ_M^{Tcrit}, σ_M^{Ccrit}, α_h^T, α_h^C, T_C^T, T_C^C and σ_Y, see Paiva *et al.* (2005). Besides, in order to consider different phase transformation kinetics for loading and unloading processes, the parameters η_n (n = 1,2,3), related to phase transformation internal dissipation, may assume different values. Therefore, $\eta_n = \eta_n^L$ if $\dot{\varepsilon} > 0$ and $\eta_n = \eta_n^U$ if $\dot{\varepsilon} < 0$.

3. Model Verification

This section presents the model verification through comparisons between the results predicted by the proposed model and experimental data reported in literature to attest its ability to describe general SMAs behavior related to subloops. Parameters are related to classical SMAs and plasticity macroscopic properties that are obtained from experimental data fitting. At first, an experimental pseudoelastic tensile test conducted by Muller & Xu (1991) on Ni-Ti wires subjected to isothermal non-proportional mechanical loading is considered. The model parameters identified for this simulation are presented in Table 1. Since plastic and compressive behaviors are not considered here, the material parameters related to these phenomena are omitted. The second experimental result for pseudoelastic tensile test

considers the research by Sittner *et al.* (1995), where an isothermal non-proportional mechanical loading is applied but this time to a Cu-Zn-Al-Mn polycrystalline SMA. Table 2 presents the model parameters considered for this simulation.

Table 1. Model parameters obtained through comparison between numerical and experimental results provided by Müller & Xu (1991) for a Ni-Ti SMA alloy.

E_A (Gpa)	E_M (GPa)	Ω_A (MPa/K)	Ω_M (MPa/K)	α^T (MPa)
6.5	4.65	0.74	0.17	1.95
L_0^T (Mpa)	L^T (MPa)	L_0^A (MPa)	L^A (MPa)	ε_R^T
36.83	230	20	180	0.052

η_1^L (kPa.tu)	η_1^U (MPa.tu)	η_3^L (MPa.s)	η_3^U (MPa.s)
89.6	77.5	89	77

T_M (K)	T_0 (K)
263	378

Table 2. Model parameters obtained through comparison between numerical and experimental results provided by Sittner *et al*. (1995) for a Cu-Zn-Al-Mn SMA alloy.

E_A (GPa)	E_M (GPa)	Ω_A (MPa/K)	Ω_M (MPa/K)	α^T (MPa)
35	27.1	0.74	0.17	0.5
L_0^T (Mpa)	L^T (MPa)	L_0^A (MPa)	L^A (MPa)	ε_R^T
36.83	169	20	109	0.0074

η_1^L (MPa.s)	η_1^U (MPa.s)	η_3^L (MPa.s)	η_3^U (MPa.s)
327	261	357	209

T_M (K)	T_0 (K)
225	285

Figure 1(a) presents a comparison between numerical and experimental results by Muller & Xu (1991), showing good agreements. On the other hand, Figure 1(b) shows that the numerical results provided by the proposed model fit well the considered experimental data by Sittner *et al*. (1995). These two comparisons attest the model's ability to represent stress-induced subloops.

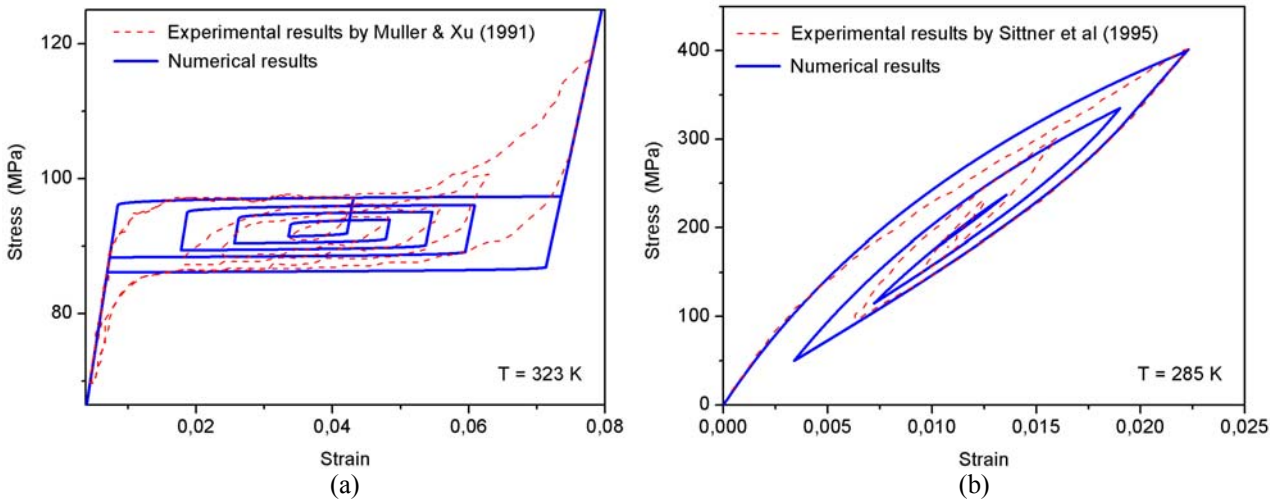

(a) (b)

Figure 1. Comparison between numerical and experimental results for pseudoelastic subloops. (a) Muller & Xu (1991). (b) Sittner *et al*.(1995).

4. Numerical Results

Numerical simulations are carried out considering various thermomechanical loadings in order to show the potentialities of the discussed model to describe SMAs thermomechanical behaviors, especially the ones related to inner subloops due to different types of incomplete phase transformations. The parameters used in the tests presented within this session were obtained through comparison between numerical simulation and experimental data presented by Tobushi *et al.* (1991), which describes tensile tests on Ni-Ti wires for three different temperatures. Figure 2 shows both numerical and experimental results in close agreement. For the sake of simplicity, a time unit (tu) is adopted to consider the loading rate. Table 3 presents the identified parameters and also some others related to the plastic behavior (Paiva *et al.*, 2005).

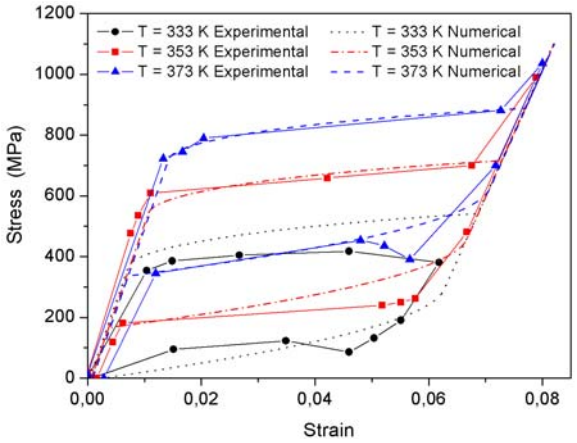

Figure 2. Comparison between numerical and experimental results by Tobushi *et al.* (1991).

Table 3. Model parameters obtained through comparison between numerical and experimental results by Tobushi *et al.* (1991).

E_A (GPa)	E_M (GPa)	Ω_A (MPa/K)	Ω_M (MPa/K)	α^T (MPa)
54	42	0.74	0.17	330
L_0^T (MPa)	L^T (MPa)	L_0^A (MPa)	L^A (MPa)	ε_R^T
0.15	41.5	0.63	185	0.0555

η_1^L (MPa.tu)	η_1^U (MPa.tu)	η_3^L (MPa.tu)	η_3^U (MPa.tu)
1	2.7	1	2.7

T_M (K)	T_A (K)	T_0 (K)
291.4	307.5	307

$\sigma_Y^{A,i}$ (GPa)	$\sigma_Y^{A,f}$ (GPa)	σ_Y^M (GPa)	η_{ci}	η_{ck}
1.5	1.0	0.5	−0.01	−0.01
K_A (GPa)	K_M (GPa)	H_A (GPa)	H_M (GPa)	T_F (K)
1.4	0.4	4	1.1	423

Three different numerical simulations are performed in order to explore the different types of subloops for pseudoelasticity, shape memory effect and phase transformation due to temperature variation. At first, the pseudoelastic behavior is presented according to the isothermal mechanical loading shown in Figure 3(a). Initially, austenite is a stable phase. The loading process induces the phase transformation $A \Rightarrow M+$. As it continues to be applied, the yield surface is reached and plastic deformation starts to take place. During unloading process, there is an elastic recovery until the reverse transformation $M+ \Rightarrow A$ begins, however, during this transformation the specimen is reloaded before it is completed. This new loading process induces a linear response before the phase transformation $A \Rightarrow M+$ occurs.

This response is related to an internal subloop. Similar cycles of loading-unloading process continue to be applied, imposing incomplete phase transformations. These processes induce other internal subloops in stress-strain curves as shown in Figure 3(b), while Figure 3(c) clearly shows the incomplete phase transformations during volumetric fractions evolution. After the complete mechanical loading removal, the irreversible plastic strain still remains.

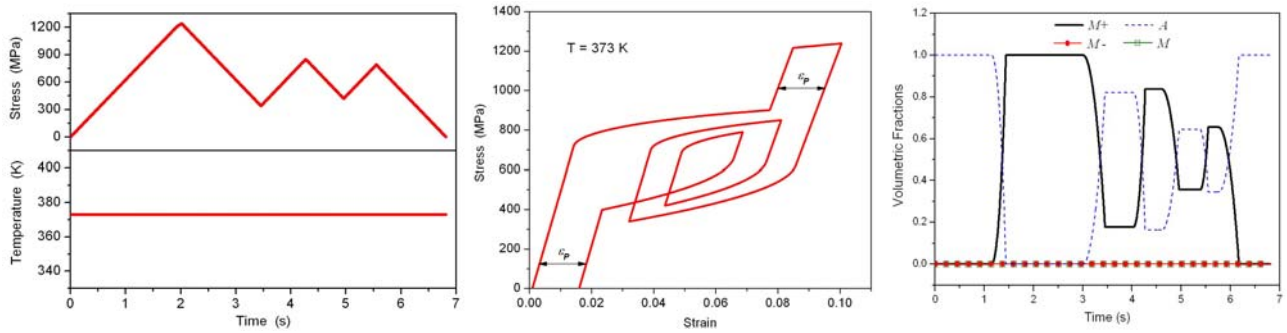

(a) (b) (c)

Figure 3. Pseudoelastic subloops.
(a) Thermomechanical loading; (b) stress-strain diagram; (c) volumetric fractions evolution.

Figure 4 considers the one-way shape memory effect. In the first part of the test, the specimen is subjected to a mechanical loading-unloading process at a constant temperature of $T = 270$ K ($T < T_M$), according Figure 4(a). Initially, twinned martensite is a stable phase. After the mechanical loading application, the specimen experiences a reorientation process from twinned martensite to detwinned martensite ($M \Rightarrow M+$). As it continues to be applied, SMA reaches the yield limit and plastic deformation starts to appear. During unloading, an elastic recovery takes place but no reverse transformation occurs resulting in an amount of strain, which corresponds to the residual strain plus a plastic strain amount. In the second part of the test, a non-proportional thermal loading with null stress level as shown in Figure 5(a) is applied, inducing incomplete phase transformation. While the specimen is heated, detwinned martensite begins to transform into austenite ($M+ \Rightarrow A$). At a certain temperature, the heating process stops and the sample is colled. The amount of austenite transforms into twinned martensite ($A \Rightarrow M$), while the detwinned martensite $M+$ remains constant. After that, the sample starts to be heated again and the twinned martensite amount becomes austenite again ($M \Rightarrow A$) describing a hysteresis loop as detailed in Figure 4(b). At a certain temperature, detwinned martensite continues to transform into austenite ($M+ \Rightarrow A$). Similar process is repeated for a higher temperature describing another hysteresis loop. At last, when the sample has fully recovered the residual strain and its structure is totally austenitic, another cooling process is imposed, transforming austenite into twinned martensite ($A \Rightarrow M$), which was the original structure before the test. After of all this thermomechanical loading is applied, the induced plastic strain still remains. Figure 4(c) shows the volumetric fractions evolution during all these phase transformation.

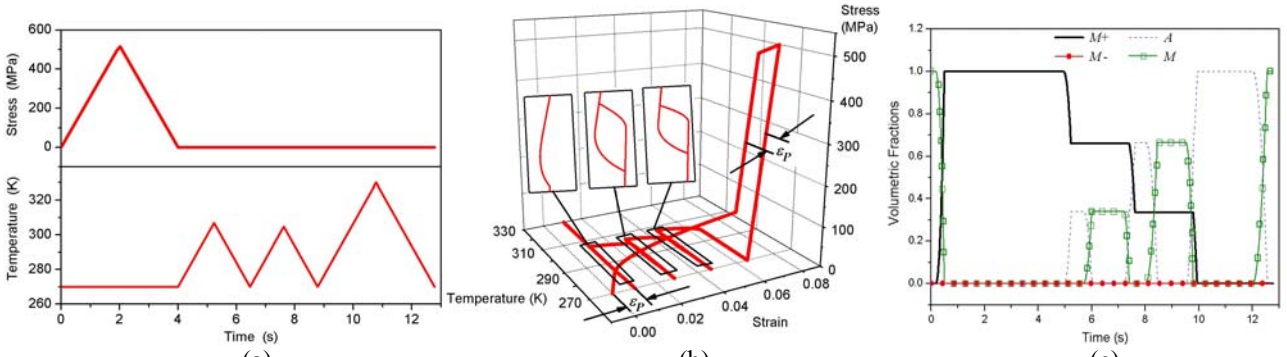

(a) (b) (c)

Figure 4. One-way shape memory effect subloops.
(a) Thermomechanical loading; (b) stress-strain-temperature diagram; (c) volumetric fractions evolution.

Now, internal subloops related to phase transformation due to temperature variation at a stress-free state are on focus. Initially, the specimen is at a high temperature where austenite is the stable phase. According to the thermomechanical loading presented in Figure 5(a), the temperature decrease causes the phase transformation from austenite to twinned martensite ($A \Rightarrow M$). Before this phase transformation finishes, the sample is heated back and experiences a linear dilatation before the reverse phase transformation ($M \Rightarrow A$) starts. Again, before phase transformation finishes, SMA is cooled and a linear contraction occurs before the remaining amount of austenite transforms into twinned martensite ($A \Rightarrow M$), describing an internal subloop, as shown in Figure 5(b). When the

structure is fully martensite, the sample is heated back promoting the $M \Rightarrow A$ transformation, bringing SMA to its original structure. The volumetric fractions evolution related to these transformations are presented in Figure 5(c).

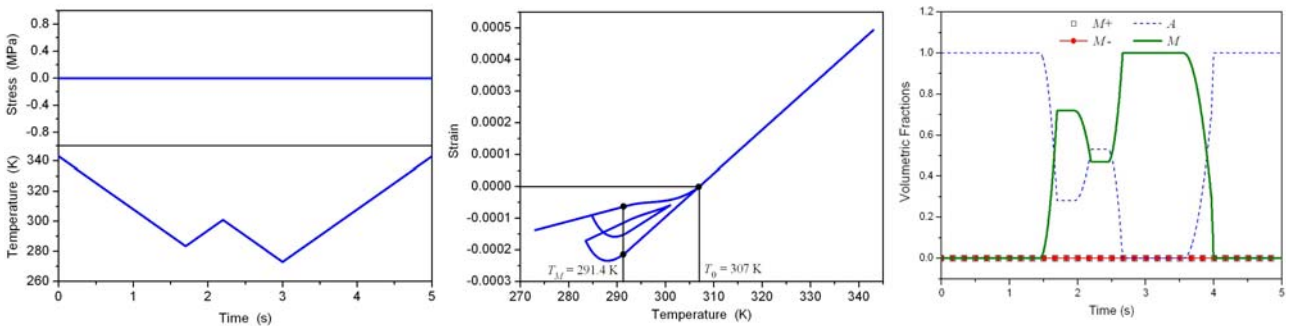

(a) (b) (c)

Figure 5. Thermal subloops.
(a) Thermomechanical loading; (b) strain-temperature diagram; (c) volumetric fractions evolution.

5. Conclusions

The present contribution discusses some features related to the description of the SMA internal subloops due to incomplete phase transformation. A constitutive model previously presented in Paiva *et al.* (2005) is employed to describe the thermomechanical behavior of SMA. Comparisons between numerical and experimental results show the capacity of the model to capture the general behavior of stress-induced inner subloops in SMAs. Moreover, a numerical investigation is carried out considering different thermomechanical loadings. This investigation shows some aspects related to the inner subloops due to incomplete phase transformation. Basically, pseudoelasticity, shape memory effect and phase transformation phenomenon due to temperature variation are evaluated. In general, the model here presented is capable to capture the thermomechanical behavior of SMA for a great variety of phenomena, showing interesting results related to incomplete phase transformations. All the results obtained for tensile tests can be obtained for compression as well.

6. Acknowledgements

The authors would like to acknowledge the support of the *Brazilian Research Council (CNPq)*.

7. References

Baêta-Neves, A.P., Savi, M.A. & Pacheco, P.M.C.L., 2004, "On the Fremond's Constitutive Model for Shape Memory Alloys", Mechanics Research Communications, Vol. 31, n. 6, pp. 677-688.

Benzaqui, H., Lexcellent, C., Chaillet, N., Lang, B. & Bourjault, A., 1997, "Experimental Study and Modeling of a TiNi Shape Memory Wire Actuator", Journal of Intelligent Material Systems and Structures, Vol. 8, pp. 619-629.

Birman, V., 1997, "Theory and Comparison of the Effect of Composite and Shape Memory Alloy Stiffeners on Stability of Composite Shells and Plates", International Journal of Mechanical Sciences, Vol. 39, n. 10, pp. 1139-1149.

Bo, Z. H. & Lagoudas, D. C., 1999, "Thermomechanical Modeling of Polycrystalline SMAs Under Cyclic Loading – Part IV: Modeling of Minor Hysteresis Loops", International Journal of Engineering Science, Vol. 37, pp. 1205-1249.

Denoyer, K. K., Erwin, R. S. & Ninneman, R. R., 2000, "Advanced Smart Structures Flight Experiments for Precision Spacecraft", Acta Astronautica, Vol. 47, pp. 389-397.

Duerig, T. M., Pelton, A., Stöckel, D., 1999, "An Overview of Nitinol Medical Applications", Materials Science and Engineering A, Vol. 273-275, pp. 149-160.

Fremond, M., 1987, "Matériaux à Mémoire de Forme", C.R. Acad. Sc. Paris, Tome 304, s. II, n. 7, pp. 239-244.

Fremond, M., 1996, "Shape Memory Alloy: A Thermomechanical Macroscopic Theory", CISM Courses and Lectures, n. 351, pp. 3-68.

Garner, L. J., Wilson, L. N., Lagoudas, D. C., Rediniotis, O. K., 2001, "Development of a Shape Memory Alloy Actuated Biomimetic Vehicle", Smart Materials & Structures, Vol. 9, n. 5, pp. 673-683.

Lagoudas, D. C., Rediniotis, O. K., Khan, M. M. 1999, "Applications of Shape Memory Alloys to Bioengineering and Biomedical Technology", Proceeding of 4th International Workshop on Mathematical Methods in Scattering Theory and Biomedical Technology, Perdika, Greece.

Lemaitre, J. & Chaboche, J.L., 1990, "Mechanics of Solid Materials", Cambridge University Press.

Machado, L. G. & Savi, M. A., 2003, "Medical Applications of Shape Memory Alloys", Brazilian Journal of Medical and Biological Research, Vol. 36, n. 6, pp. 683-691.

Machado, L. G. & Savi, M. A., 2002, "Odontological Applications of Shape Memory Alloys", Revista Brasileira de Odontologia, Vol. 59, n. 5, pp. 302-306 (in portuguese).
Muller, I. & Xu, H., 1991, "On the Pseudo-elastic Hysteresis", Acta Metallurgical Materials, Vol. 39, n. 3, pp. 263-271.
Nishimura, F., Watanabe, N. & Tanaka, K., 1997, "Stress-Strain-Temperature Hysteresis and Martensite Start Line in an Fe-Based Shape Memory Alloy", Materials Science and Engineering, Vol. A238, pp. 367-376.
Ortin, J., 1991, "Partial Hysteresis Cycles in Shape Memory Alloys: Experiments and Modelling", Journal de Physique IV, Vol. 1, pp. C4-65–C4-70.
Ortin, J. & Delaey, L., 2002, "Hysteresis in Shape Memory Alloys", International Journal of Non-Linear Mechanics, Vol. 37, pp. 1275-1281.
Pacheco, P. M. C. L. & Savi, M. A., 2000, "Modeling and Simulation of a Shape Memory Release Device for Aerospace Applications", Revista de Engenharia e Ciências Aplicadas.
Paiva, A., Savi, M. A., Braga, A. M. B. & Pacheco, P. M. C. L., 2005, "A Constitutive Model for Shape Memory Alloys Considering Tensile-Compressive Asymmetry and Plasticity", International Journal of Solids and Structures, Vol. 42, n. 11-12, pp. 3439-3457.
Paiva, A., 2004, "Modeling of Thermomechanical Behavior of Shape Memory Alloys", Ph.D. Thesis, PUC-Rio, Department of Mechanical Engineering, 113 pp. (in portuguese).
Rogers, C. A., 1995, "Intelligent Materials", Scientific American, September, pp. 122-127.
Savi, M. A., Paiva, A., Baêta-Neves, A. P. & Pacheco, P. M. C. L., 2002, "Phenomenological Modeling and Numerical Simulation of Shape Memory Alloys: A Thermo-Plastic-Phase Transformation Coupled Model", Journal of Intelligent Material Systems and Structures, Vol. 13, n. 5, pp. 261-273.
Sittner, P., Hara, Y., Tokuda, M., 1995, "Experimental Study on the Thermoelastic Martensitic Transformation in Shape Memory Alloy Polycrystal Induced by Combined External Forces", Metallurgical and Materials Transactions A, Vol. 26A, pp. 2923-2935.
Tanaka, K. & Nagaki, S., 1982, "Thermomechanical Description of Materials with Internal Variables in the Process of Phase Transformation", Ingenieur – Archiv., Vol. 51, pp. 287-299.
Tanaka, K., Nishimura, F. & Tobushi, H. (1994), "Phenomenological Analysis on Subloops in Shape Memory Alloys Due to Incomplete Transformations", Journal of Intelligent Material Systems and Structures, Vol. 5, pp. 387-493.
Tanaka, K., Nishimura, F., Hayashi, T., Tobushi, H. & Lexcellent, C., 1995, "Phenomenological Analysis on Subloops and Cyclic Behavior in Shape Memory Alloys Under Mechanical and/or Thermal Loads", Mechanics of Materials, Vol. 19, pp. 281-292.
Tanaka, K., Nishimura, F., Matsui, M., Tobushi, H. & Lin, P.-H., 1996, "Phenomenological Analysis on Plateaus on Stress-Strain Hysteresis in TiNi Shape Memory Alloy Wires", Mechanics of Materials, Vol. 24, pp. 19-30.
van Humbeeck, J., 1999, "Non-medical Applications of Shape Memory Alloys", Materials Science and Engineering A, Vol. 273-275, pp. 134-148.
Webb, G., Wilson, L., Lagoudas, D.C. & Rediniotis, O., 2000, "Adaptive Control of Shape Memory Alloy Actuators for Underwater Biomimetic Applications", AIAA Journal, Vol. 38, n. 2, pp. 325-334.